INVESTIGATION OF NUCLEAR RADIUS PARAMETER USING ENERGY DIFFERENCES OF MIRROR NUCLEI

Ismail F. Jiad[†], Wasan Z. Majeed

Department of Physics, College of Science, University of Baghdad
Baghdad, Iraq

Received 4 September 2024, accepted 9 January 2025,
published online 26 February 2025

The mirror energy difference is a mainly noticeable in isospin symmetry breaking, containing important facts about the nuclear structure. From the examination of these differences, several nuclear structure properties can be studied. Thus, in this work, the binding energy differences of mirror nuclei with $A = 23$, 25, and 27 are investigated in terms of the Hartree–Fock (HF) calculations with Skxta, Sly4, and Skxs25 Skyrme parameterizations. β^+-decay energy $E(\beta^+)$ and the nuclear radius parameter of ^{23}Na, ^{25}Mg, and ^{27}Al nuclei together with their mirror nuclei ^{23}Mg, ^{25}Al, and ^{27}Si are calculated, followed by a regular investigation of the binding energy difference. The calculated values of the nuclear radius parameter are in good agreement with those derived from mirror nuclei experiments. In addition, the ground-state density distributions, form factors, root mean square radii, and the relationship between the proton skin of a nucleus and the difference between the proton radii of mirror nuclei are studied. In general, a linear relationship between the proton skin and the difference in the proton radii between the mirror pair nuclei was observed

DOI:10.5506/APhysPolB.56.2-A4

1. Introduction

In nuclear physics, it is important to study the mirror nuclei which have the interchanged number of protons and neutrons, since it directly addresses the isospin symmetry idea described by Heisenberg in 1932 [1]. Interest in mirror nuclei has become very important since the development of radioactive ion beams (RIBS), therapeutic medical, nuclear medicine, and other applications. Researchers have widely theoretically and experimentally studied mirror nuclei for light and heavy nuclei [2]. In addition, a great interesting feature of investigating the mirror nuclei is the Coulomb energy difference which provides a stringent test for nuclear models [3]. Also, the change in Coulomb energy of mirror nuclei has been studied to measure the value of nuclear radius [4].

[†] Corresponding author: `Ismail@sc.uobaghdad.edu.iq`

The nuclear radius is the basic parameter used to describe the structure of the nucleus and considered as a key to study the static properties of nuclei [5]. Various theoretical studies are conducted to examine the properties of mirror nuclei [6–10]. The Hartree–Fock method with Skyrme forces is extensively used for studying nuclear characteristics such as binding energy, root mean square (r.m.s.) radii, and skin thickness [11–14].

Boso *et al.* [15] used the Mirror Energy Differences (MEDs) in up to high spin, as a direct result of isospin symmetry breaking to study the ^{23}Mg–^{23}Na mirror nuclei. They chose the MED in their work to provide valuable information on a variety of nuclear structural features. Mohammed and Majeed [16] calculated the ground-state properties of two pairs of mirror nuclei ^{17}Ne–^{17}N and ^{23}Al–^{23}Ne using shell-model calculations. They investigated the relationship between the proton skin of a nucleus and the difference between the proton radii of mirror pairs.

The current work aims to determine the value of the nuclear radius parameter from the mirror energy differences of (^{23}Na–^{23}Mg), (^{25}Mg–^{25}Al) and (^{27}Al–^{27}Si) nuclei. Besides, the nuclear properties such as the ground-state density distributions, form factors, root mean square radii, and proton skin of these nuclei are investigated in terms of the Hartree–Fock (HF) calculations with Skxta, Sly4, and Skxs25 Skyrme parameterizations.

2. Theory

The expectation value of the HF Hamiltonian of the system is given by [17]

$$\langle \phi_{\mathrm{HF}}|\hat{H}|\phi_{\mathrm{HF}}\rangle = \sum_{i=1}^{A}\langle \phi_i|\hat{T}|\phi_i\rangle + \frac{1}{2}\sum_{ij}^{A}\langle \phi_i\phi_j|\vec{\nu}(ij)|\phi_i\phi_j\rangle\,, \tag{1}$$

where $\vec{\nu}(ij)$ contains all parts of nucleon–nucleon forces. These forces consist of some two-body terms together with a three-body term [18]

$$\hat{V}_{\mathrm{Skyrme}} = \sum_{i<j} V_{ij}^{(2)} + \sum_{i<j<k} V_{ijk}^{(3)} \tag{2}$$

with

$$\begin{aligned} V_{ij}^{(2)} &= t_0(1+x_0 p_\sigma)\delta\left(\vec{r}\right) + \frac{1}{2}t_1\left[\delta\left(\vec{r}\right)\vec{k}^{\,2} + \vec{k}^{\sim 2}\delta\left(\vec{r}\right)\right] \\ &\quad + t_2\vec{k}^{\sim 2}\delta\left(\vec{r}\right)\vec{k} + iW_0\left(\vec{\sigma}_i - \vec{\sigma}_j\right)\vec{k}\times\delta\left(\vec{r}\right)\vec{k}\,, \end{aligned} \tag{3}$$

$$V_{ijk}^{(3)} = t_3\delta\left(\vec{r}_i - \vec{r}_j\right)\delta\left(\vec{r}_j - \vec{r}_k\right)\,. \tag{4}$$

The relative momentum operators are, respectively, $\vec{k} = (\nabla_i - \nabla_j)/2i$ acting to the right and $\vec{k}^{\sim 2} = -(\nabla_i - \nabla_j)/2i$ acting to the left. The neutron, proton or charge densities in the Skyrme–Hartree–Fock (SHF) theory are given by [19]

$$\rho_g\left(\vec{r}\right) = \sum_{\beta \in g} w_\beta \psi_\beta^+\left(\vec{r}\right)\psi_\beta\left(\vec{r}\right)\,, \tag{5}$$

where g is used for proton, neutron, and charge densities, ψ_β is the single-particle wave function of the state β, and w_β represents the occupation probability of the state β. The charge form factor, $F(q)$, is obtained from the charge density by the Fourier–Bessel transform [20]

$$F(q) = 4\pi \int\limits_0^\infty r^2 j_0(qr)\rho_c(r)\mathrm{d}r\,, \tag{6}$$

where q is the momentum transfer. The r.m.s. radii of neutron, proton, and charge densities can be calculated using Eq. (5) with the following formula [21]:

$$\left\langle r_g^2\right\rangle^{1/2} = \left[\frac{\int r^2\rho_g(r)\mathrm{d}r}{\rho_g(r)\mathrm{d}r}\right]^{1/2}\,, \qquad g = n, p, c\,. \tag{7}$$

The neutron-skin thickness $\varDelta\langle r^2\rangle_n^{1/2}$ and the proton-skin thickness $\varDelta\langle r^2\rangle_p^{1/2}$ are related to the difference between the neutron $\langle r^2\rangle_n^{1/2}$ and proton $\langle r^2\rangle_p^{1/2}$ r.m.s. radii for the nucleus and their mirror as [9, 22]

$$\varDelta\left\langle r^2\right\rangle_n^{1/2} = \left\langle r^2\right\rangle_n^{1/2} - \left\langle r^2\right\rangle_p^{1/2}\,, \tag{8}$$

$$\varDelta\left\langle r^2\right\rangle_p^{1/2} = \left\langle r^2\right\rangle_p^{1/2} - \left\langle r^2\right\rangle_n^{1/2}\,, \tag{9}$$

$$\varDelta\left\langle r^2\right\rangle_{\mathrm{mirror}}^{1/2} = \left\langle r^2\right\rangle_p^{1/2}(N,Z) - \left\langle r^2\right\rangle_p^{1/2}(Z,N)\,. \tag{10}$$

Equation (10) represents the important method to determine neutron and proton skin using charge radii of mirror pair's nuclei. The difference in binding energy of a pair of mirror nuclei, (Z,N) and (N,Z), is expressed as [23]

$$\Delta B(Z,N) = B(Z,N) - B(N,Z)\,. \tag{11}$$

The $\Delta B(Z,N)$ value is determined by the Coulomb displacement energies as

$$\Delta B(Z,N) = a_{\mathrm{C}}\frac{Z^2 - N^2}{A^{1/3}} = -a_{\mathrm{C}}\Delta Z A^{2/3}\,, \tag{12}$$

where $\Delta Z = N - Z$.

3. Results and discussion

The binding energy difference, β^+-decay energy $E(\beta^+)$, nuclear radius parameter, r.m.s. radii, density distributions, form factors, and skin thickness are calculated for three pairs of mirror nuclei (^{23}Na–^{23}Mg), (^{25}Mg–^{25}Al), and (^{27}Al–^{27}Si) in the framework of HF calculations with selected Skyrme forces (Skxta, Sly4, and Skxs25). The binding energy difference ($\Delta B(Z,N)$), β^+-decay energy $E(\beta^+)$, and the value of the nuclear radius parameter (r_0) are presented in Table 1 with the available experimental data.

Table 1. The calculated values $\Delta B(Z,N)$, $E(\beta^+)$, and r_0 parameter.

Pairs of mirror nuclei	Skyrem forces	$\Delta B(Z,N)$ [MeV]	$E(\beta^+)$ [MeV]	r_0 [fm]
^{23}Mg–^{23}Na	Skxta	4.899	3.877	1.42
	Sly4	4.410	3.388	1.58
	Skxs25	4.957	3.935	1.4
	Exp. [24]	4.836	3.034(3)	—
^{25}Al–^{25}Mg	Skxta	5.25	4.228	1.4
	Sly4	4.772	3.750	1.54
	Skxs25	5.335	4.313	1.38
	Exp. [24]	5.059	3.254(4)	—
^{27}Si–^{27}Al	Skxta	5.596	4.574	1.38
	Sly4	5.136	4.114	1.51
	Skxs25	5.707	4.685	1.36
	Exp. [24]	5.595	3.790(10)	—

From this table, it is clear that the calculated $\Delta B(Z,N)$ of three pairs of mirror nuclei using Skxta are closer to the experimental data than other parameterizations. It is evident from the result that the difference in binding energy comes from the fact that the binding energy of nuclei with an excess of protons is smaller than the binding energy of mirror nuclei with an excess of neutrons due to the stronger repulsive Coulomb interaction. Thus, this interaction plays the main role in the binding energy of mirror nuclei and it is required to have a sensible Coulomb energy. The results showed also that the calculated values of β^+-decay energy $E(\beta^+)$ of mirror nuclei and the experimental data correlate extremely well when the Sly4 parameterization is used. For the sake of completeness of the comparison, the nuclear radius parameter, r_0 is evaluated. This value is in good agreement with those derived from mirror nuclei experiments — 1.4 fm [4] and differs from the value measured from the experimental data by electron scattering and μ-mesonic atoms, $r_0 = 1.2$ fm [4].

The calculated proton, neutron, and matter r.m.s. radii of the three pairs of mirror nuclei are listed and compared with the available experimental data in Table 2. From Table 2, it is clear that the calculated r.m.s. is in good agreement with the experimental data for all parameterization. These parameters (Skxta, Sly4, Skxs25) were randomly selected from several parameters in the Hartree–Fock so that we could see their correlation with the experimental results.

Table 2. The values of r.m.s. proton $\langle r_p^2\rangle^{1/2}$, neutron $\langle r_n^2\rangle^{1/2}$, and matter $\langle r_m^2\rangle^{1/2}$ radii in fm for (^{23}Na–^{23}Mg), (^{25}Mg–^{25}Al), and (^{27}Al–^{27}Si) mirror nuclei.

r.m.s. [fm]		^{23}Na	^{23}Mg	^{25}Mg	^{25}Al	^{27}Al	^{27}Si
	Skxta	2.884	2.948	2.940	2.997	2.994	3.045
	Sly4	2.928	2.986	2.973	3.023	3.013	3.055
$\langle r_p^2\rangle^{1/2}$	Skxs25	2.940	3.016	2.984	3.052	3.025	3.087
	Exp. [25]	2.81	3.12	2.89	—	—	—
	Skxta	2.905	2.853	2.954	2.908	3.001	2.960
	Sly4	2.946	2.898	2.982	2.943	3.014	2.981
$\langle r_n^2\rangle^{1/2}$	Skxs25	2.958	2.898	2.994	2.942	3.028	2.982
	Exp. [2, 25]	3.04±0.05	3.08	3.02±0.47	—	2.9	3.02±0.47
	Skxta	2.895	2.903	2.947	2.955	2.998	3.004
	Sly4	2.937	2.944	2.978	2.985	3.014	3.020
$\langle r_m^2\rangle^{1/2}$	Skxs25	2.949	2.960	2.989	3.000	3.027	3.036
	Exp. [2, 26]	2.93±0.03	2.96±0.14	2.96±0.25	2.98	3.03	2.9

From the proton radii of the nucleus and its mirror, one can determine the relationship between the proton skin of a nucleus and the difference between the proton radii of the mirror pair as shown in Table 3. The related proton-skin thickness is found to be greater than the neutron-skin thickness due to the proton's Coulomb repulsion. Additionally, Table 3 shows that the difference between two proton radii becomes larger in the presence of the Coulomb repulsion, whereas the neutron skin becomes smaller due to the increase in the proton radius.

Table 3. Predicted proton skins $\Delta\langle r_p^2\rangle^{1/2}$, neutron skins $\Delta\langle r_n^2\rangle^{1/2}$ of corresponding mirror nuclei and $\Delta\langle r_{\text{mirror}}^2\rangle^{1/2}$ mirror in fm.

Nucleus	$\Delta\langle r_p^2\rangle^{1/2}$			Mirror	$\Delta\langle r_n^2\rangle^{1/2}$			$\Delta\langle r_{\text{mirror}}^2\rangle^{1/2}$		
	Skxta	Sly4	Skxs25		Skxta	Sly4	Skxs25	Skxta	Sly4	Skxs25
^{23}Mg	0.095	0.088	0.118	^{23}Na	0.021	0.018	0.018	0.064	0.058	0.076
^{25}Al	0.089	0.08	0.11	^{25}Mg	0.014	0.009	0.01m	0.057	0.05	0.068
^{27}Si	0.085	0.074	0.105	^{27}Al	0.007	0.001	0.003	0.051	0.042	0.062

Figure 1 shows the calculated results of the proton and neutron skins as a function of mass number (A) for Skxta, Sly4, and Skxs25 Skyrme parameterizations. The predictions of all parameterizations describe the decrease of the proton and neutron skin with increasing A.

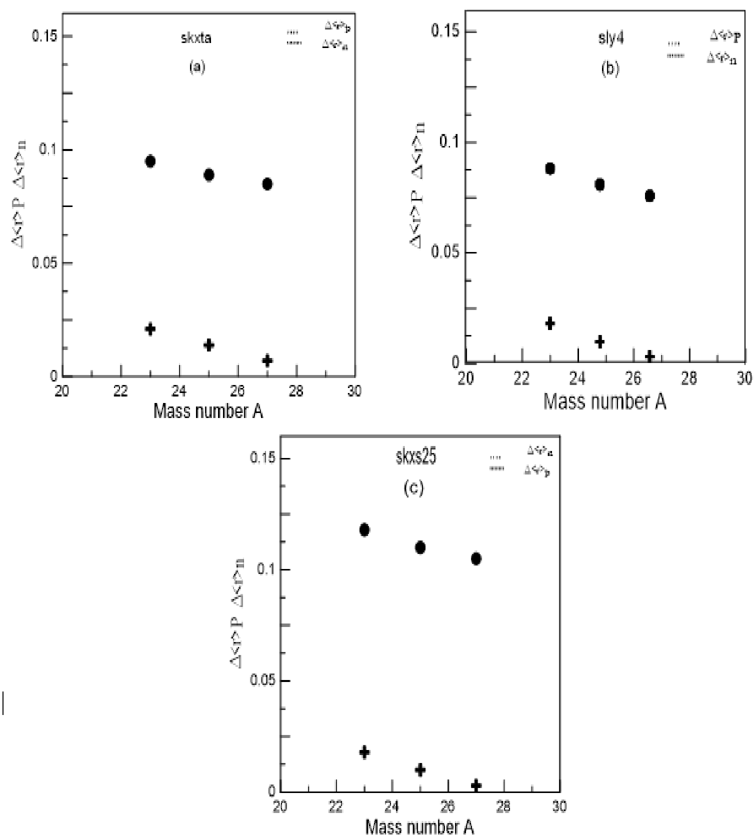

Fig. 1. The calculated proton and neutron skins with (a) Skxta, (b) Sly4, and (c) Skxs25 as a function of A.

In order to study the differences between ground-state properties of the mirror nuclei, charge and neutron density distributions of three pairs of mirror nuclei are displayed in Figs. 2, 3, and 4 using the HF calculations with Skxta, Sly4, and Skxs25 parameterizations. The red solid and dashed curves in these figures represent the charge and neutron density, respectively, for the ^{23}Mg, ^{25}Al, and ^{27}Si nuclei. The blue solid and dashed represent the charge and neutron density, respectively, for the ^{23}Na, ^{25}Mg, and ^{27}Al nuclei. These figures show that there is an asymmetry in the proton density of the ^{23}Mg, ^{25}Al, and ^{27}Si nuclei and the neutron density of their mirror nuclei due to the fact that the Coulomb interaction pushes out the density of the protons relative to neutrons.

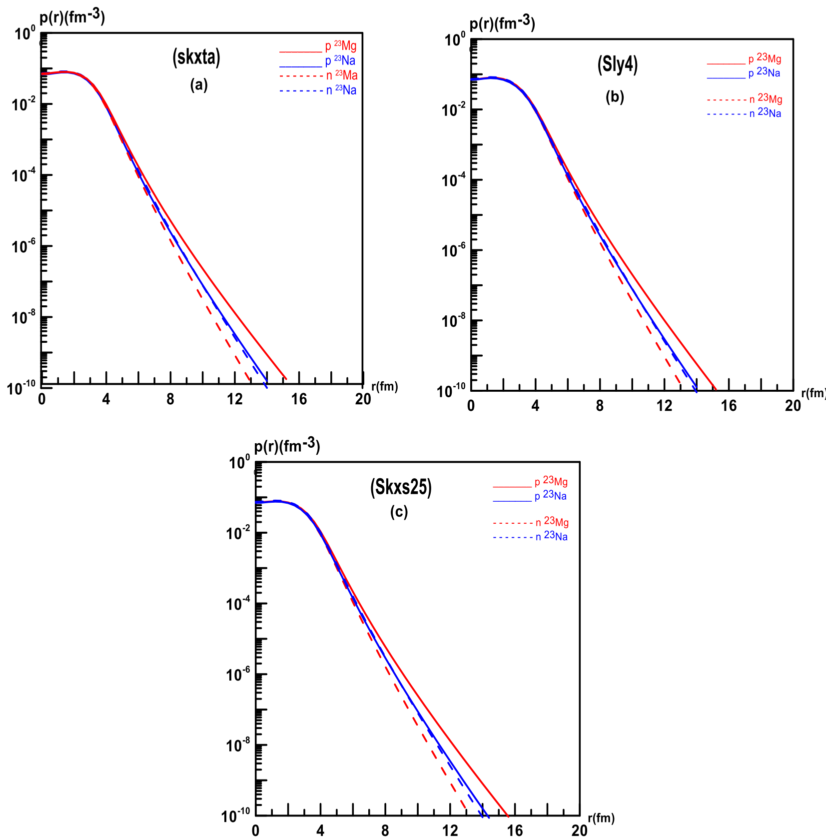

Fig. 2. Charge and neutron density distribution for mirror nuclei ^{23}Na–^{23}Mg using (a) Skxta, (b) Sly4, and (c) Skxs25.

Figure 2 represents the density distribution of protons and neutrons for the mirror pair. As we observe, the density distribution of protons has a longer tail than that of neutrons, which is attributed to the Coulomb repulsion between protons, causing them to be pushed outward.

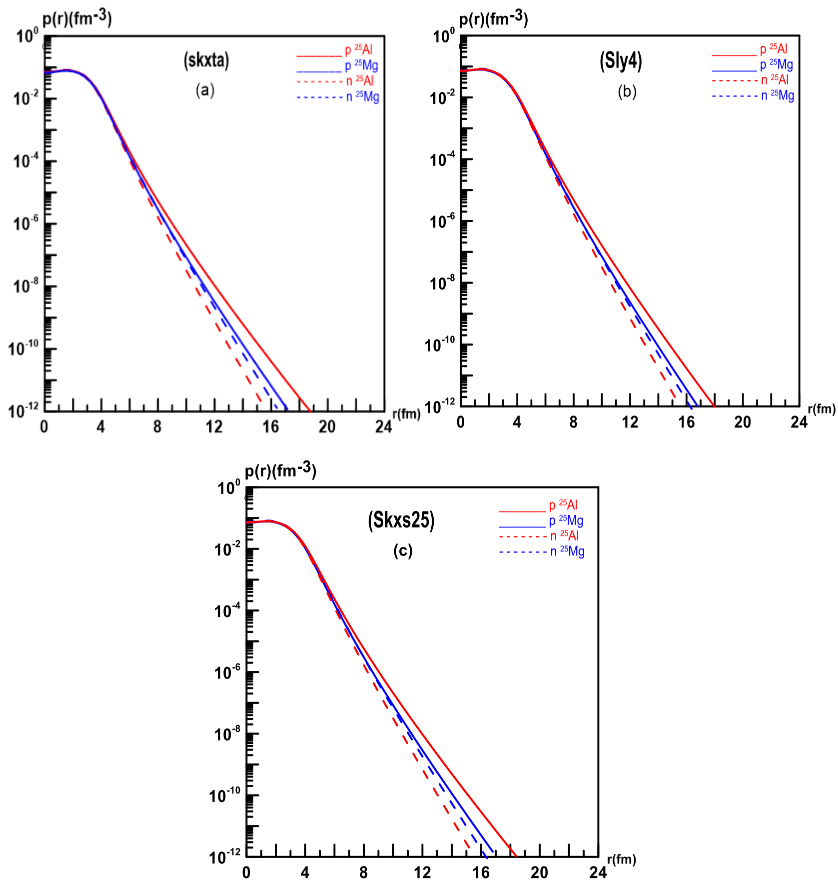

Fig. 3. Charge and neutron density distribution for mirror nuclei ^{25}Al–^{25}Mg using (a) Skxta, (b) Sly4, and (c) Skxs25.

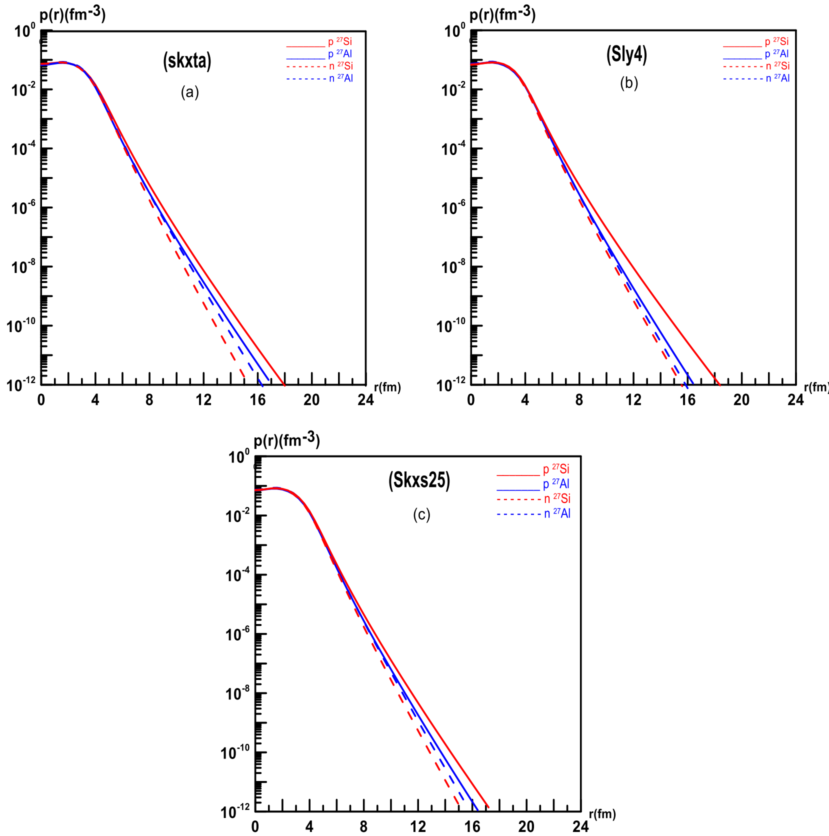

Fig. 4. Charge and neutron density distribution for mirror nuclei ^{27}Si–^{27}Al using (a) Skxta, (b) Sly4, and (c) Skxs25.

The matter density distributions of three pairs of mirror nuclei are displayed in Figs. 5, 6, and 7 with the available experimental data. In these figures, the red curves are the calculated matter density of the ^{23}Mg, ^{25}Al, and ^{27}Si nuclei and the blue curves represent the matter density of their mirror obtained with Skxta, Sly4, and Skxs25 parameterizations. The filled circles are the experimental data. It is evident from Fig. 7 that the calculated matter density distribution for all parameterizations is in good accordance with that of the fitted density. The density distributions of the ^{23}Mg, ^{25}Al, and ^{27}Si nuclei shown in these figures have longer tails than that of their mirror nuclei.

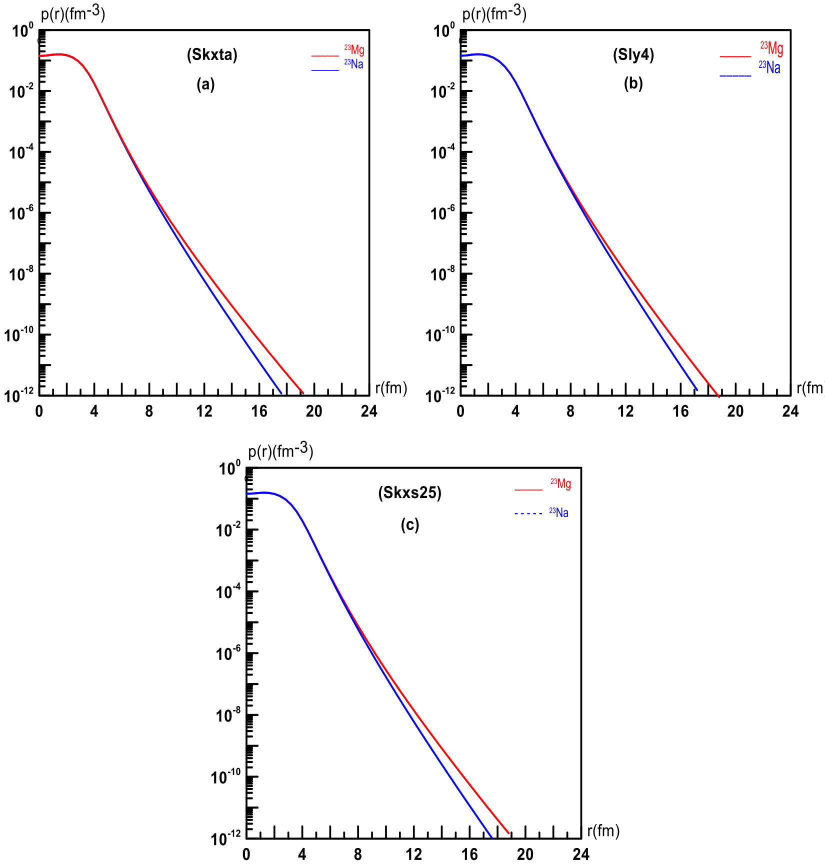

Fig. 5. Matter density distribution of mirror nuclei ^{23}Mg–^{23}Na using (a) Skxta, (b) Sly4, and (c) Skxs25.

Figure 5 illustrates the relationship between the matter density distribution and the nuclear radius of the nuclear pair (^{23}Na–^{23}Mg) calculated using the Hartree–Fock method with three (Skxta, Sly4, and Skxs25) parameterizations. It is observed that there is a difference in the nuclear pair that starts at 8 femtometers and increases gradually with the increase in the nuclear radius. This variation is a result of the differences in the number of protons and neutrons, which causes a disparity in the effects of the Coulomb repulsion, thereby influencing the overall distribution of matter.

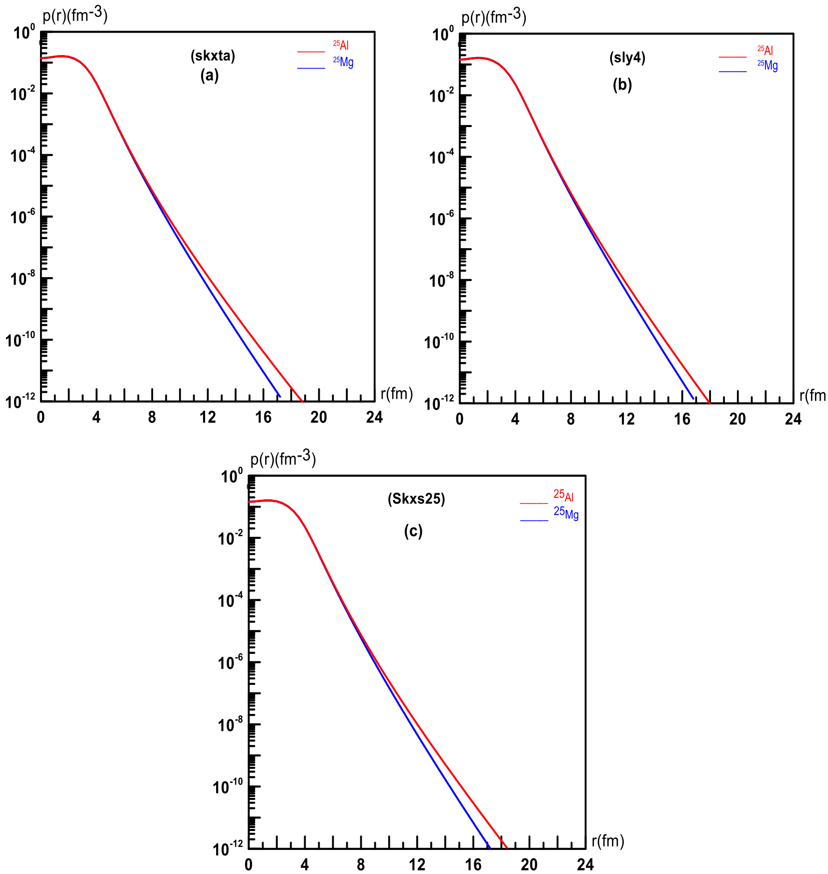

Fig. 6. Matter density distribution for mirror nuclei ^{25}Al–^{25}Mg using (a) Skxta, (b) Sly4, and (c) Skxs25.

Figure 6 illustrates the density distribution of the pair ^{25}Mg–^{25}Al using the Hartree–Fock method with three parameters. As shown in the figure, the ^{25}Al has a longer tail than ^{25}Mg due to the Coulomb repulsion effect, as it has a greater number of protons than ^{25}Mg. At the center of the nucleus, we observe that the density distribution is higher, and then the density gradually decreases with the increase in nuclear radius.

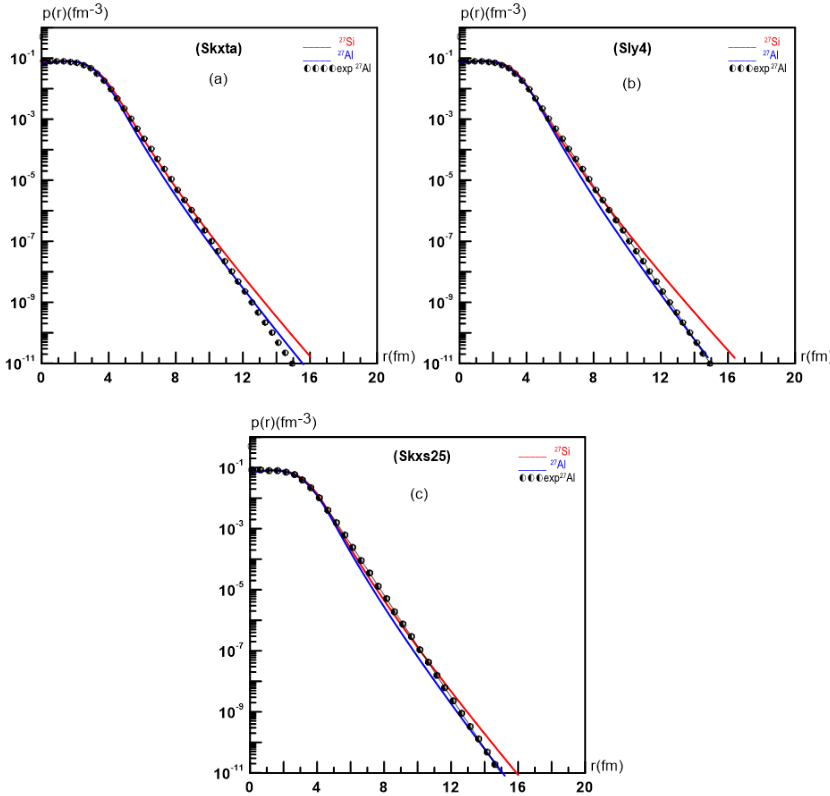

Fig. 7. Matter density distribution for mirror nuclei ^{27}Si–^{27}Al using (a) Skxta, (b) Sly4, and (c) Skxs25. The dotted symbols are the experimental data of Ref. [26].

Figure 7 represents the density distribution of the pair ^{27}Si–^{27}Al mirror nuclei, according to the Hartree–Fock method calculated using three parameters and compared with experimental data. One can see that the theoretical data align well with the experimental values.

Finally, elastic form factors of these pairs of mirror nuclei are calculated as shown in Fig. 8. We present the computed C_0 form factor utilizing Skxta parameterization for ^{23}Mg, ^{25}Al, and ^{27}Si nuclei (red curve) and ^{23}Na, ^{25}Mg, and ^{27}Al nuclei (blue curve) to compare the results of the form factor of the nuclei with those of their mirror nuclei, as shown in the figure. The filled circles are the experimental data [26]. The figure shows that the charge form factors of the pairs of mirror nuclei are similar since the ground-state charge density is connected with the C_0 form factor.

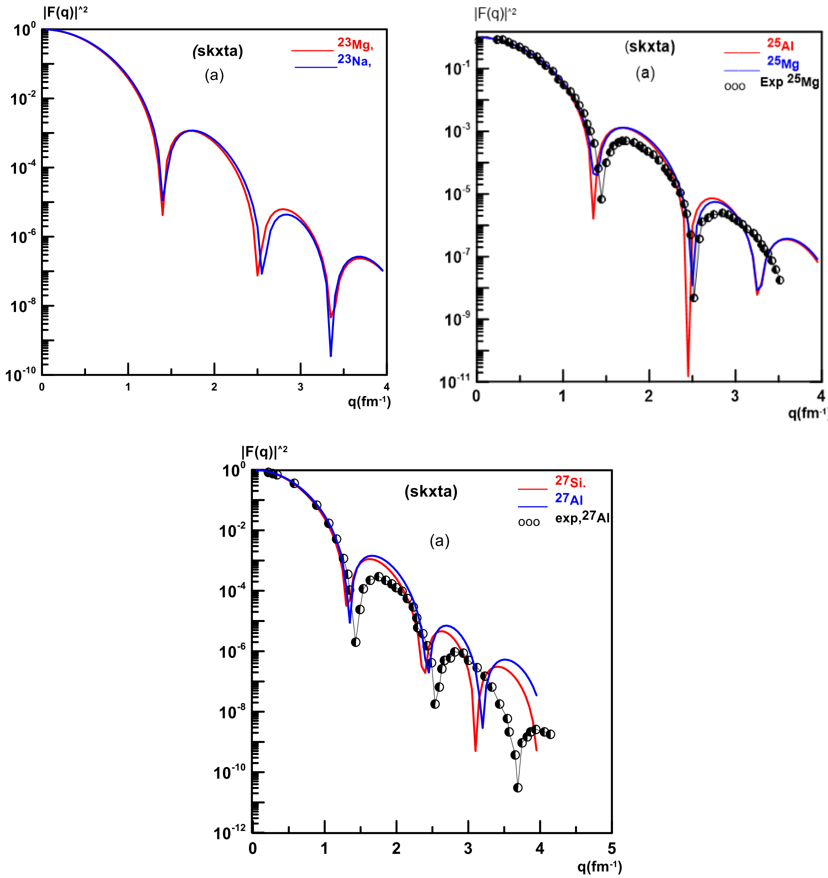

Fig. 8. Elastic form factors (a) for ^{23}Mg–^{23}Na, (b) for ^{25}Al–^{25}Mg, (c) for ^{27}Si–^{27}Al nuclei. The dotted symbols show the experimental data for ^{25}Mg and ^{27}Al [26].

Figure 8 represents curves of the form factors for three pairs calculated using the Skxta parameter with the Hartree–Fock method diverging from the experimental data. This deviation could be attributed to the increasing mass number of the nuclei, which leads to a decrease in accuracy as the mass number rises. In addition, we observe that the curves representing the form factors for the Skxta parameter are in good agreement with the experimental data at a transferred momentum of $q = 1.5$ fm^{-1}.

4. Conclusions

In this work, we systematically calculated the mirror energy difference, the β^+-decay energy, and nuclear radius parameter as well as the ground-states properties of three pairs of mirror nuclei, namely (^{23}Na–^{23}Mg), (^{25}Mg–^{25}Al), and (^{27}Al–^{27}Si) using the Hartree–Fock (HF) calculations with Skxta, Sly4, and Skxs25 Skyrme parameterizations.

The results revealed that the difference in binding energy comes from the fact that the binding energy of nuclei with an excess of protons is smaller than the binding energy of mirror nuclei with an excess of neutrons due to the stronger repulsive Coulomb interaction. It is evident from the result that the calculated values of β^+-decay energy and nuclear radius parameter are in good agreement with the experimental data. The result showed also that each pair of mirror nuclei has different size in terms of their nuclear size, and these differences get linearly larger with increasing mass number A. Furthermore, a linear relationship was observed between the proton skin of a nucleus and the difference between the proton radii of the corresponding mirror pair.

REFERENCES

[1] H. Jian *et al.*, «β-Delayed γ Emissions of ^{26}P and Its Mirror Asymmetry», *Symmetry* **13**, 2278 (2021).

[2] A. Ozawa, T. Suzuki, I. Tanihata, «Nuclear size and related topics», *Nucl. Phys. A* **693**, 32 (2001).

[3] B.K. Agrawal *et al.*, «Coulomb energy differences in mirror nuclei revisited», *Phys. Rev. C* **64**, 243051 (2001).

[4] A. Adamu, F.M. Mustapha, M.K. Dikwa, «Determination of Nuclear Radius Parameter from β^+ Transformation Energy of Mirror Nuclei», *J. Sci. Technol. Res.* **1**, 137 (2019).

[5] I. Angeli, «Manifestation of Non-traditional Magic Nucleon Numbers in Nuclear Charge Radii», *Acta Phys. Debrecina* **XLVII**, 7 (2013).

[6] R.H. Harith, S. Hameed, «Study of the Symmetry Energy and the Nuclear Equation of State for ^{13}O–^{13}B and ^{13}N–^{13}C Mirror Nuclei», *Iraqi J. Phys.* **21**, 24 (2023).

[7] R.A. Mohammed, W.Z. Majeed, «Differences in Ground State Properties of Some Mirror Nuclei», *Phys. Atom. Nuclei* **86**, 77 (2023).

[8] B.N. Giv, S. Mohammadi, «Calculating Energy Levels in ^{49}Mn/^{49}Cr Mirror Nuclei with OXBASH Code», *Comput. Biol. Bioinform.* **5**, 70 (2017).

[9] F. Sammarruca, «Proton Skins, Neutron Skins, and Proton Radii of Mirror Nuclei», *Front. Phys.* **6**, 1 (2018).

[10] S. Liu, H.K. Jia, T.F. Wang, Y.B. Qian, «Binding energies of proton-rich nuclei determined from their mirror pairs», *Chinese Phys. C* **47**, 014105 (2023).

[11] R.A. Radhi, A.A. Alzubadi, N.F. Latooffi, «Investigation of the Nuclear Structure of $^{174-206}$Hg Isotopes Using Skyrme–Hartree–Fock Method», *Iraqi J. Sci.* **56**, 738 (2015).

[12] R.A. Radhi, A. Ridha, W. Majeed, «Comparison between shell model and self-consistent mean field calculations for ground charge density distributions and elastic form factors of ^{12}C and ^{16}O nuclei», *Indian J. Phys.* **89**, 723 (2015).

[13] W. Majeed, «Investigation of density and form factor of some F isotopes using Hartree–Fock and shell model calculations», *Iraqi J. Phys.* **14**, 158 (2019).

[14] O.A. Alswaidawi, A.A. Alzubadi, «Hamiltonian sensitivity in calculating the electromagnetic moments and electroexcitation form factor for the sd nuclei using shell model with Skyrme–Hartree–Fock», *Int. J. Mod. Phys. E* **32**, 3250020 (2023).

[15] A. Bosol *et al.*, «Isospin Symmetry Breaking in Mirror Nuclei ^{23}Mg–^{23}Na», *Acta Phys. Pol. B* **48**, 313 (2017).

[16] R.A. Mohammed, W.Z. Majeed, «Exotic Structure of ^{17}Ne–^{17}N and ^{23}Al–^{23}Ne Mirror Nuclei», *East Eur. J. Phys.* **2022**, 72 (2022).

[17] Li Guo-qiang, «Skyrme Forces and Their Applications in Low Energy Nuclear Physics», *Commun. Theor. Phys.* **13**, 457 (1990).

[18] P. Ring, P. Schuck, «The Nuclear Many Body Problem», *Springer*, Berlin, Heidelberg 1980.

[19] H. Aytekin *et al.*, «Investigation of the Ground State Features of Some Excotic Nuclei by Using Effective Skyrme Interaction», *Turk. J. Phys.* **32**, 181 (2008).

[20] Li Guo-Qiang, «A systematic study of nuclear properties with Skyrme forces», *J. Phys. G: Nucl. Part. Phys.* **17**, 1 (1991).

[21] M. Wang *et al.*, «The Ame2012 atomic mass evaluation», *Chinese Phys. C* **36**, 1603 (2012).

[22] M.K. Gaidarov *et al.*, «Proton and neutron skins and symmetry energy of mirror nuclei», *Nucl. Phys. A* **1004**, 122061 (2020).

[23] P. Bączyk *et al.*, «Isospin-symmetry breaking in masses of $N \simeq Z$ nuclei», *Phys. Lett. B* **778**, 178 (2018).

[24] Center For Photonuclear Experiments Data (CDFE), available from `http://cdfe.sinp.msu.ru/services/index.en.html`

[25] S. Ahmad, A.A. Usmani, Z.A. Khan, «Matter radii of light proton-rich and neutron-rich nuclear isotopes», *Phys. Rev. C* **96**, 6 (2017).

[26] H. De Vries, C.W. De Jager, C. De Vries, «Nuclear charge-density-distribution parameters from elastic electron scattering», *Atom. Data Nucl. Data* **36**, 495 (1987).